Int. J. Electrochem. Sci., 16 **(2021)** Article ID: 210525, doi: 10.20964/2021.05.18

International Journal of
ELECTROCHEMICAL
SCIENCE
www.electrochemsci.org

Structure, Magnetization Behaviors and Corrosion Resistance of MnBi/NdFeB Nanocomposite Magnet

Yuanhao TU[1], *Hangfu Yang*[1,*], *Hengjing Zhang*[2], *Minxiang Pan*[1], *Nengjun Yu*[1], *Heng Xu*[2], *Qiong Wu*[1,*], *Hongliang Ge*[1]

[1] Magnetism key laboratory of Zhejiang Province, China Jiliang University, Hangzhou 310018, China
[2] Zhejiang Fangyuan Test Group Co., LTD, Hangzhou, 310018, China
[*]E-mail: yang_hangfu@yahoo.com (Hangfu Yang); wuqiong@cjlu.edu.cn (Qiong Wu)

Received: 28 January 2021 / *Accepted:* 16 Febrary 2021 / *Published:* 31 March 2021

The MnBi/NdFeB nanocomposite alloys have been fabricated by the low energy ball milling. The influence of NdFeB content on the microstructure and magnetic properties of these nanocomposite alloys were investigated. The magnetic properties results show that the saturation magnetization (M_s) of $Mn_{55}bi_{45}/Nd_2Fe_{14}B$ nanocomposite alloys increases with the increase of $Nd_2Fe_{14}B$ content, which is due to the high saturation magnetization of $Nd_2Fe_{14}B$. The magnetization reversal behavior by the study of the $\delta M(H)$ and the ratio of H_r/H_c prove that the MnBi/NdFeB nanocomposite alloys with different NdFeB content have stronger exchange coupling effect. Besides, a remarkably improvement in electrochemical stability for the MnBi/NdFeB nanocomposite magnet with the NdFeB added.

Keywords: Permanent; Corrosion; Magnetic properties; Recoil-loop

1. INTRODUCTION

As one of the important research directions to improve the performance of permanent magnet materials, nanocomposite dual phase permanent magnet materials have always been the research hotspot of magnetic materials [1-5]. Rare earth permanent magnet materials have excellent magnetic properties, but its application temperature range is narrow. MnBi non-rare earth permanent magnet has higher coercivity and positive temperature coefficient of coercivity, which helps to improve the application temperature range of magnetic materials. With the exploitation of rare earth resources, the cost of rare earth permanent magnet is higher, while MnBi non-rare earth permanent magnet is higher and the cost of raw materials is low. At present, hard soft two-phase nanocomposite permanent magnetic materials have been reported, which mainly include four types: $Fe_3B/Nd_2Fe_{14}B$, $Nd_2Fe_{14}B/\alpha$-Fe, $Sm_2(Fe,M)_{17}C_y/\alpha$-Fe and SmCo/α-Fe [6-10]. However, there are few studies on hard two-phase

nanocomposite permanent magnetic materials, so it has high research value and application value to nanocomposite magnets [11-14].

To further enhance the magnetic properties of the MnBi/NdFeB nanocomposite alloys, the MnBi/NdFeB nanocomposite alloys are fabricated by the low energy ball milling were investigated in the present work. Meanwhile, the effect of different NdFeB contents on the magnetic properties, microstructures, magnetization behavior and corrosion resistance of the MnBi/NdFeB nanocomposite alloys were also discussed in detail.

2. EXPERIMENTAL PART

The $Nd_2Fe_{14}B$ magnetic powder was obtained by grinding the oxide scale of the magnetic block according to the nominal composition of $Nd_2Fe_{14}B$, then crushing and grinding in the glove box, and screening through 100 meshes. According to the nominal composition of $Mn_{55}bi_{45}$, the purity of 99.9 wt% Mn and 99.9 wt% metal Bi were mixed according to the atom ratio, the vacuum degree was pumped to 3×10^{-3} Pa, and then argon was poured to 0.05 Pa. Finally, the $Mn_{55}bi_{45}$ ingot was melted by arc in argon atmosphere, and the alloy was melted for 6 times to ensure uniform composition. The ingot was then pre-annealed at 290 ℃ for 24 hours, then crushed and ground in glove box, and screened with 100 mesh to obtain $Mn_{55}bi_{45}$ grinding magnetic powder. The two-phase powders were prepared with varying $Mn_{55}bi_{45}$: $Nd_2Fe_{14}B$ ratios from 1:0 to 1:1 in weight. The 50 ml ethanol was added as solvent, 10% PVP was added as surfactant and put into low energy ball milling for 3 hours. The as-milled MnBi/NdFeB powders were firstly pressed into cubes in the glove box under Ar atmosphere, and then pressed at 100 MPa under cold isostatic pressure.

The phase composition was examined by X-ray diffraction (XRD). Magnetic measurements were accomplished by using a vibrating-sample magnetometer (VSM). Polarization curves were determined with a PARSTAT 2273 advance electrochemical system. Each measurement was performed using two electrode cells consisting of $SmCo_5$/α-Fe alloys working electrode and Pt counter electrode. Ally experiments were conducted in 2.5 wt.% NaCl aqueous solution with scan rate of 2 mV/s along the direction from the negative potential to the positive one.

3. RESULTS AND DISCUSSION

Figure 1 shows the XRD patterns of the MnBi/NdFeB nanocomposite alloys as a function of different NdFeB contents. It can be seen that with the increase of $Nd_2Fe_{14}B$ content, the diffraction peak positions of the Bi-phase, LTP MnBi phase, $Nd_2Fe_{14}B$ phase and α-Fe phase do not change, which indicates that the phase composition of $Mn_{55}bi_{45}$ and $Nd_2Fe_{14}B$ is not changed after a certain period of ball milling. Moreover, the LTP MnBi phase still has a strong diffraction peak and the relative content remains at a high value, which means that the addition of PVP-assisted low energy ball milling is effective to reduce the decomposition of LTP MnBi phase. Meanwhile, as the reason of the

diffraction peaks of Bi-phase and LTP MnBi phase are too strong, the peaks of $Nd_2Fe_{14}B$ phase and α-Fe phase appear when the addition of $Nd_2Fe_{14}B$ reaches to 50%.

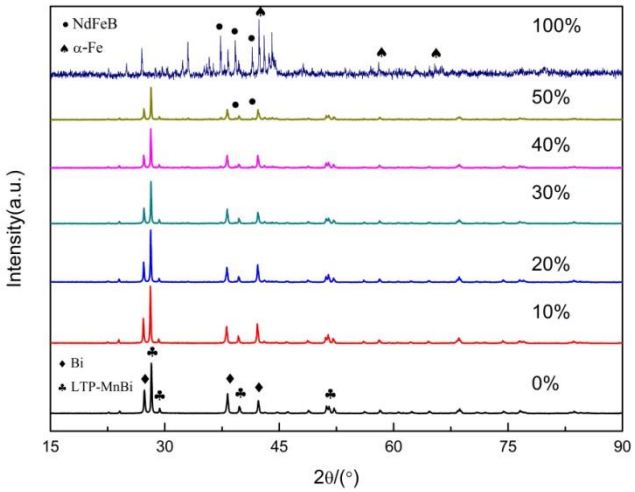

Figure 1. XRD patterns of the MnBi/NdFeB nanocomposite alloys as a function of different NdFeB contents.

Figure 2 (a) presents the hysteresis loops of the MnBi/NdFeB nanocomposite alloys as a function of different NdFeB contents. It shows that the hysteresis loops of all samples are single hard magnetic phase behavior, and the curve basically does not appear concave or bee waist shape. Meanwhile, the intrinsic coercivity (H_{cj}) has little change with the increase of $Nd_2Fe_{14}B$ content, while compared with the $Mn_{55}bi_{45}$ magnet without $Nd_2Fe_{14}B$, the intrinsic coercivity obvious decreases from 6500 Oe to ~ 2000 Oe, as it can be seen from the Fig. 2 (b) of the variations in saturation magnetization (M_s) and intrinsic coercivity (H_{cj}) on the MnBi/NdFeB nanocomposite alloys with different NdFeB contents. In addition, saturation magnetization (M_s) of $Mn_{55}bi_{45}/Nd_2Fe_{14}B$ nanocomposite alloys increases with the increase of $Nd_2Fe_{14}B$ content, which is due to the high saturation magnetization of $Nd_2Fe_{14}B$. The magnetic properties of the single-phase $Mn_{55}Bi_{45}$ and $Nd_2Fe_{14}B$ magnets are also shown in Table 1. As one can see, the magnetic properties of MnBi/NdFeB nanocomposite magnets are obviously different from that of single-phase magnet, indicating that the magnetic properties of the hybrid magnets are sensitive to the ratio of the two hard phases and confirming the existence of two-phase exchange-coupling interaction in the MnBi/NdFeB nanocomposite magnets, similar phase equilibrium characteristics were also observed in the SmCo/a-Fe nanocomposite alloys [7].

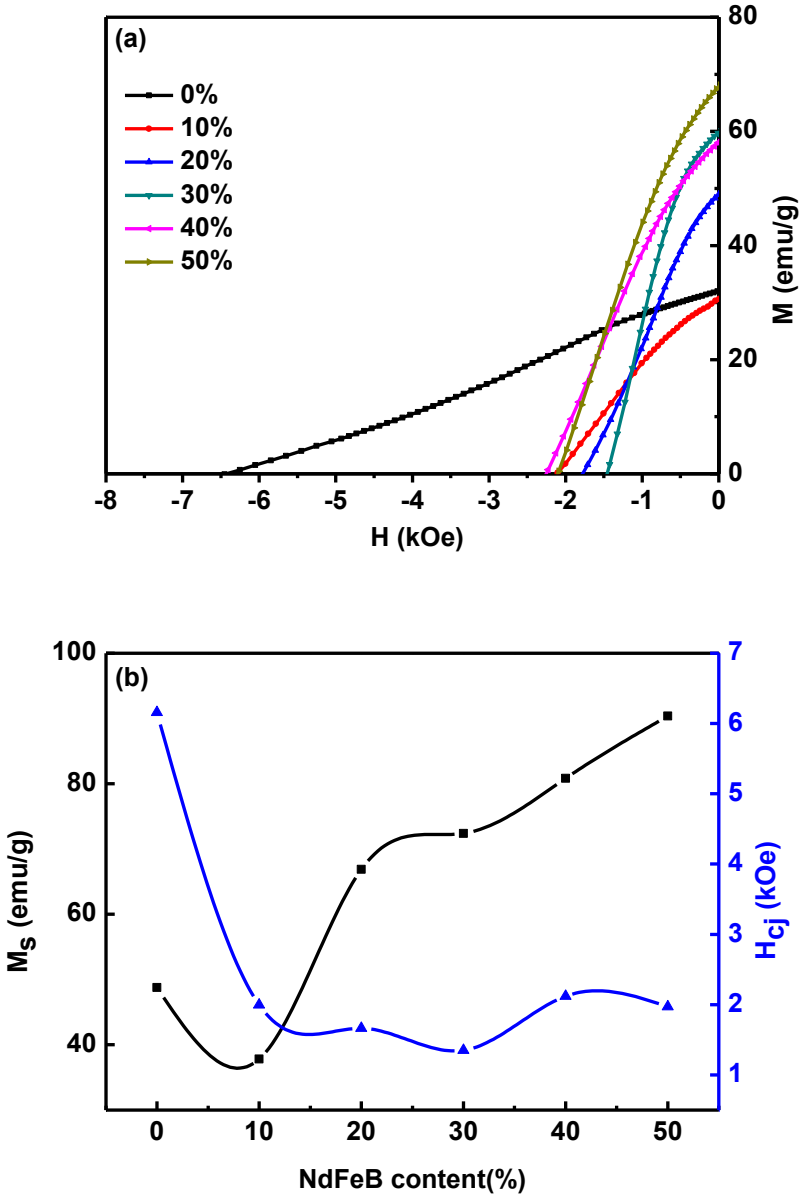

Figure 2. (a) Hysteresis loops of the MnBi/NdFeB nanocomposite alloys as a function of different NdFeB contents. (b) Variations in saturation magnetization (M_s) and intrinsic coercivity (H_{cj}) on the MnBi/NdFeB nanocomposite alloys with different NdFeB contents.

Table 1. Saturation magnetization (M_s), intrinsic coercivity (H_{cj}) of the single-phase $Mn_{55}Bi_{45}$ and $Nd_2Fe_{14}B$ magnets.

Magnets	M_s (*emu/g*)	H_{cj} (*kOe*)
$Mn_{55}Bi_{45}$	58.4	2.35
$Nd_2Fe_{14}B$	135.6	2.15

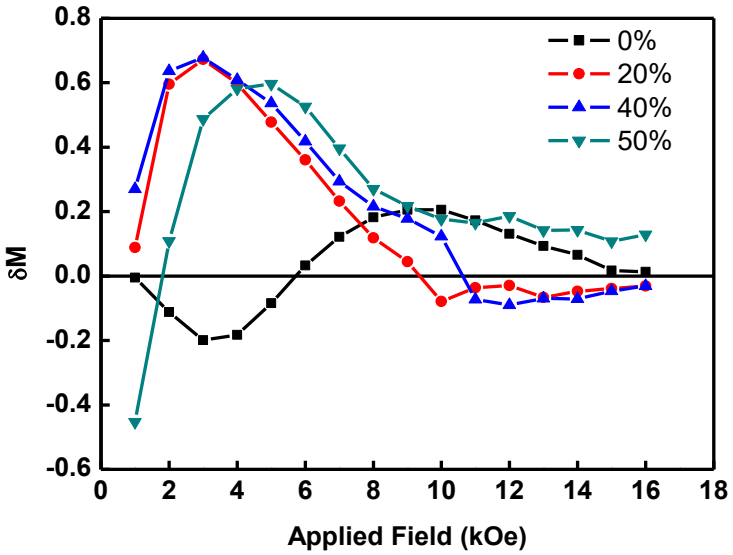

Figure 3. The variation of δM with applied magnetic field for the MnBi/NdFeB nanocomposite alloys as a function of different NdFeB contents.

In order to study the exchange coupling effect and the magnetization reversal behaviors in the MnBi/NdFeB nanocomposite alloys, the inter-granular exchange coupling is estimated by using the δM plot, which can be defined as $\delta M(H) = [M_d(H) - M_r(H)+2 M_r(H)]/M_r(H)$. Here, $M_r(H)$ is the remanent magnetization measured by applying the gradually increasing magnetization field H along the positive direction from the demagnetization state, while $M_d(H)$ is the saturation magnetization of the sample in the opposite direction, and then applying and removing the gradually increasing magnetization field along the positive direction in turn [15-18]. Figure 3 shows the variation of δM with applied magnetic field for the MnBi/NdFeB nanocomposite alloys as a function of different NdFeB contents. It can see that MnBi/NdFeB nanocomposite magnets with different NdFeB contents show different changing trends. This is mainly due to when the nanocomposite sample is in demagnetization state at the beginning and the applied magnetic field H is lower than the impossible nucleation field H_N, the exchange coupling between the two-phase composite magnetic particles will inhibit the magnetization reversal of the sample. Meanwhile, it shows that in the MnBi/NdFeB nanocomposite alloys with different NdFeB content, the δM values of the samples with 20%, 40% and 50% NdFeB content are significantly higher than those of the sample without NdFeB content, which proves that the MnBi/NdFeB nanocomposite alloys with different NdFeB content have stronger exchange coupling effect. For the MnBi sample without NdFeB content, the δM value is negative, which indicates that there is a strong stray field in the sample. The main reason is that the magnetic particle size heterogeneity leads to the magnetostatic exchange coupling effect in the magnetic material, which leads to the low coercivity.

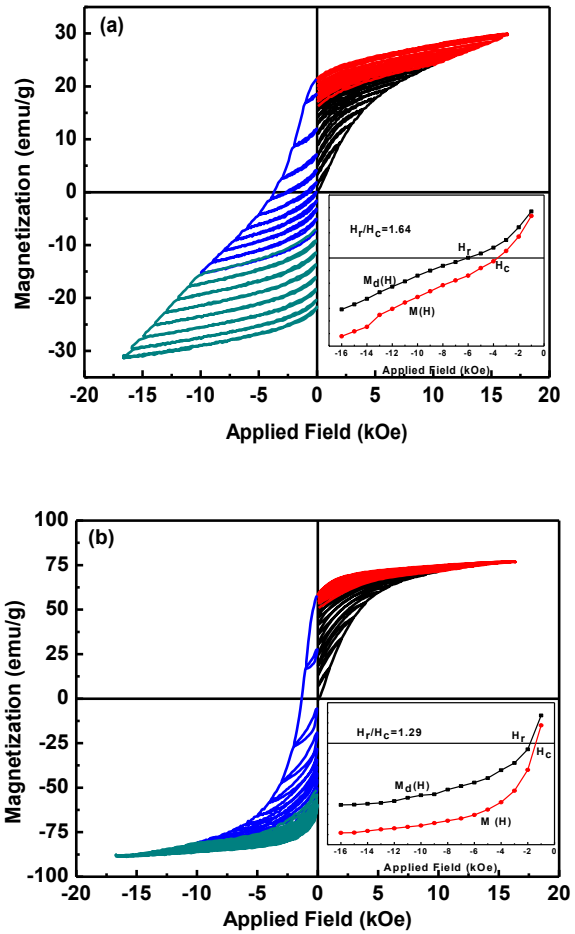

Figure 4. The recoil loops of the hysteresis curves on the applied reversal field of the MnBi/NdFeB nanocomposite alloys for the NdFeB content at (a) free and (b) 40%. The magnetization $M(H)$ and the dc demagnetization remanence $M_d(H)$ curves as a function of μ_0 times the applied reversal field are given in the inset also.

To get further insight to the different magnetic behavior of these samples, the mechanism of the exchange-coupled MnBi/NdFeB nanocomposite alloys is discussed as follows. Fig. 4 show the recoil loops of the hysteresis curves on the applied reversal field of the MnBi/NdFeB nanocomposite alloys for the NdFeB content at (a) free and (b) 40%. As seen, the recoil loops of the two samples are not closed, and this phenomenon often occurs in the composite phase of nanocomposite materials. This is because some particles or nanocrystals in the dual phase composite magnetic materials have irreversible magnetization reversal under the action of counter magnetic field, thus forming this kind of non recoil loops. Meanwhile, the reversible susceptibility appears in MnBi/NdFeB nanocomposite alloy, which indicates that MnBi/NdFeB nanocomposite alloy exhibit remanence enhancement and strong exchange coupling, which is a typical "exchange-spring" phenomenon in composite magnets. Meanwhile, for the further understand the inter-granular exchange coupling, the plots of $M_d(H)$ and the $M(H)$ curves are given in the inset also. According to the previous theoretical model of Kneller and Hawing [19-21], the ratio of H_r to H_c in the single-phase magnet without exchange coupling is 1.09. It can be seen from the figure that even the ratio of H_r/H_c in the magnet without NdFeB is 1.64, which

indicates that the exchange coupling effect is relatively weak, while the H_r/H_c of MnBi/NdFeB nanocomposite powder with 40% NdFeB content is 1.29, which further indicates that the exchange coupling performance of MnBi/NdFeB nanocomposite alloy is improved. Similar behavior was observed by Wu et al. previously [22].

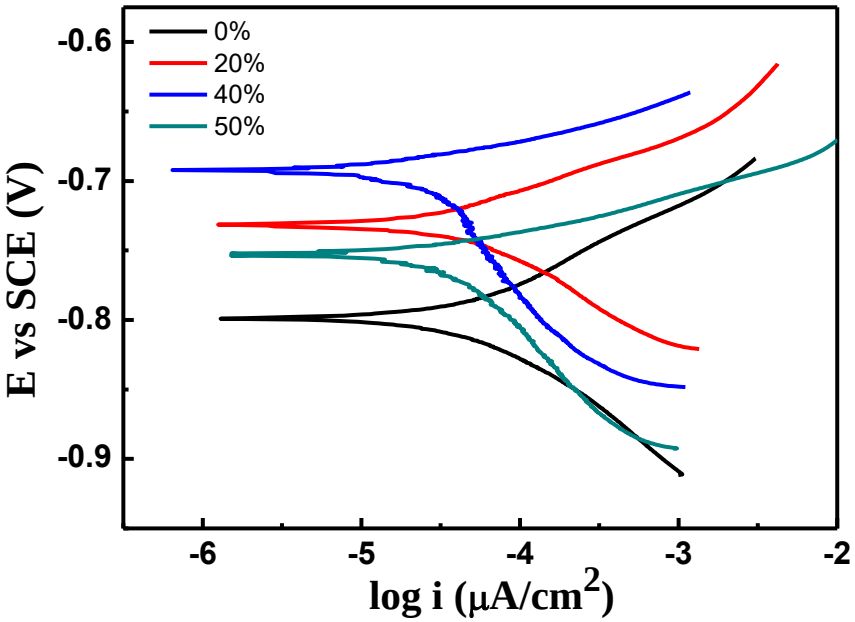

Figure 5. Polarization curves of the MnBi/NdFeB nanocomposite alloys as a function of different NdFeB contents in 2.5 wt.% NaCl aqueous solutions.

Table 2. The corrosion potential E_{corr} and corrosion current density i_{corr} of the MnBi/NdFeB nanocomposite alloys as a function of different NdFeB contents in 2.5 wt.% NaCl aqueous solutions.

Magnets	E_{corr}(V)	i_{corr}(μA/cm^2)
free	-0.799	63.32
20%	-0.732	39.82
40%	-0.693	17.95
50%	-0.753	25.11

Fig. 5 shows the potentiodynamic polarization curves of the MnBi/NdFeB nanocomposite alloys as a function of different NdFeB contents in 2.5 wt.% NaCl aqueous solutions. Meanwhile, the corrosion potential E_{corr} and corrosion current density i_{corr} of the MnBi/NdFeB nanocomposite alloys are obtained according to the potentiodynamic polarization curves and illustrated in Table 2. It can be seen that the corrosion potential E_{corr} is -0.799 V and the corrosion current density i_{corr} is 63.32 μA/cm^2 for the NdFeB-free sample, while the corrosion potential E_{corr} is increased to -0.693 V and the corrosion current density i_{corr} is decreased to 17.95 μA/cm^2 for the 40% NdFeB content MnBi/NdFeB

nanocomposite alloy. The lower corrosion current density i_{corr} and higher corrosion potential E_{corr} for the MnBi/NdFeB nanocomposite alloys with the NdFeB content at 40% are remarkably improved by the addition of the NdFeB. The present study demonstrated that the magnetic properties can be improved and the exchange coupling interaction can be enhanced in the MnBi/NdFeB nanocomposite alloys with proper NdFeB added. Meanwhile, the corrosion resistance of these magnets can be also improved.

4. CONCLUSION

In this study, the effect of NdFeB content on the magnetic properties, microstructures, magnetization behavior and corrosion resistance of the MnBi/NdFeB nanocomposite alloys were discussed in detail. The magnetic properties results show that the saturation magnetization (M_s) of $Mn_{55}bi_{45}/Nd_2Fe_{14}B$ nanocomposite alloys increases with the increase of $Nd_2Fe_{14}B$ content, which is due to the high saturation magnetization of $Nd_2Fe_{14}B$. The magnetization reversal behavior by the study of the $\delta M(H)$ and the ratio of H_r/H_c prove that the MnBi/NdFeB nanocomposite alloys with different NdFeB content have stronger exchange coupling effect. The lower corrosion current density i_{corr} and higher corrosion potential E_{corr} for the MnBi/NdFeB nanocomposite alloys with the NdFeB content at 40% are remarkably improved by the addition of the NdFeB.

ACKNOWLEDGEMENT
This research was supported by National Key Research and Development Project (No. 2019YFF0217205), the Key R&D Program of Zhejiang Province of China (Nos. 2021C01190, 2020C05013 and 2021C01191) and the Zhejiang Provincial Natural Science Foundation of China (Nos. LGC20E010004 and LY21A040006).

References

1. J.J. Croat, J.F. Herbst, R.W. Lee, F.E. Pinkerton, *Appl. Phys. Lett.,* 44 (1984) 148.
2. C.Y. Hu, M.X. Pan, Q. Wu, H.L. Ge, X.M. Wang, Y.C. Lu, P.Y. Zhang, *J. Rare. Earth.,* 34 (2016) 61.
3. Z.B. Li, B.G. Shen, M. Zhang, F.X. Hu, J.R. Sun, *J. Alloys Compd.,* 628 (2015) 325.
4. M.X. Pan, P.Y. Zhang, X.J. Li, H.L. Ge, Q. Wu, Z.W. Jiao, T.T. Liu, *J. Rare. Earth.,* 28 (2010) 399.
5. M. Sagawa, S. Fujimura, N. Togawa, H. Yamamoto, Y. Mutsuura, *J. Appl. Phys.,* 55 (1984) 2083.
6. X. Li, Z. M. Ren, Y. Fautrelle, *Mater. Lett.,* 60 (2006) 3379.
7. J.T. Li, M.X. Pan, Y.D. Yu, H.L. Ge, Q. Wu, *Int. J. Electrochem. Sci.,* 13 (2018) 8897.
8. M.X. Pan, H. Xu, Z. Li, X.H. Tan, X.L. Hou, Y. Gu, P.Y. Zhang, *Aip. Adv.,* 8 (2018) 115320.
9. Y. Yang, J.W. Kim, P.Z. Si, H.D. Qian, Y.H. Shin, X.Y. Wang, J.H. Park, O.L. Li, Q. Wu, H.L. Ge, C.J. Choi, *J. Alloys Compd.,* 769 (2018) 813.
10. M.X. Pan, P.Y. Zhang, H.L. Ge, Q. Wu, N.J. Yu, *Mater. Sci. Tech-Lond.,* 30 (2014) 832.
11. S. Kim, H. Moon, H. Jung, S.-M. Kim, H.-S. Lee, C.-Y. Haein, W. Lee, *J. Alloys Compd.,* 708 (2017) 1245.
12. M.X. Pan, P.Y. Zhang, Q. Wu, H.L. Ge, *Int. J. Electrochem. Sci.,* 11 (2016) 2659.
13. K. Kang, L.H. Lewis, A. R. Moodenbaugh, *J. Appl. Phys.,* 97 (2005) 10k302.

14. S.Y. Zhang, P.Y. Zhang, H.C Jiang, Y.J. Shi, N.J. Yu, H.L. Ge, *J. Magn.*, 19 (2014) 205.
15. G. K. Williamson, *Acta. Metall.*, 1 (1953) 23.
16. M.X. Pan, P.Y. Zhang, H.L. Ge, Q. Wu, N.J. Yu, *J. Rare. Earth.*, 31 (2013) 262.
17. M.X. Pan, P.Y. Zhang, H.L. Ge, Q. Wu, *Mater. Technol.*, 31 (2016) 580.
18. Y.B. Yang, X.G. Chen, S. Guo, A.R. Yan, Q.Z. Huang, M.M. Wu, D.F. Chen, Y.C. Yang, J.B. Yang, *J. Magn. Magn. Mater.*, 330 (2013) 106.
19. E.P. Wohlfarth, *J. Appl. Phys.*, 29 (1958) 595.
20. M.X. Pan, P.Y. Zhang, H.L. Ge, H.F. Yang, Q. Wu, S.H. Hua, H.C. Jiang, *Rare. Metal. Mat. Eng.*, 8 (2013) 1685.
21. J. Lyubina, K.H. Müller, M. Wolf, U. Hannemann, *J. Magn. Magn. Mater.*, 322 (2010) 2948.
22. Q. Wu, J.T. Li, P.Y. Zhang, M.X. Pan, H.L. Ge, *Int. J. Electrochem. Sci.*, 14 (2019) 4318.